

# Behaviour of $S$ -Wave poles Near Threshold and the Scalar Meson Nonet Below 1 GeV

Eef van Beveren <sup>a</sup> and George Rupp <sup>b</sup>

<sup>a</sup> *Centro de Física Teórica, Departamento de Física, Universidade, P3004-516 Coimbra, Portugal, (eef@teor.fis.uc.pt)*

<sup>b</sup> *Centro de Física das Interações Fundamentais, Instituto Superior Técnico, Edifício Ciência, P1049-001 Lisboa Codex, Portugal, (george@ajax.ist.utl.pt)*

November 13, 2018

## Abstract

We describe the behaviour at threshold of  $S$ -wave poles of the scattering matrix within a four-parameter model for non-exotic meson-meson scattering. This model accommodates all non-exotic mesons, hence also the light scalar mesons, as resonances and bound states characterised by complex singularities of the scattering amplitude as a function of the total invariant mass.

The majority of the full  $S$ -matrix mesonic poles stem from an underlying confinement spectrum. However, the light scalar mesons  $K_0^*(830)$ ,  $a_0(980)$ ,  $f_0(400-1200)$ , and  $f_0(980)$  do not, but instead originate in  $^3P_0$ -barrier semi-bound states. We show that the behaviour of the corresponding poles is identical at threshold.

## Introduction

In a theory with quarks and mesons one can study strong interactions through meson-meson scattering. Observed spectra may be interpreted in terms of quark-antiquark or more complicated systems [1]. Necessarily, spectra must be confirmed in several different experiments, and compiled in spectroscopic tables. Then, for a lowest-order approximation of strong interactions, confinement models may be constructed. Their usefulness can be measured by the model's achievements when adjusting its parameters to experiment[2].

For further refinements of strong-interaction models, there are several possible directions. One way is to reanalyse experiments in order to adjust the data to new insights [3], in particular when popular models [4] are not capable of reproducing specific experimental results [5, 6, 7, 8]. Another way is to adapt the model by including more sophisticated interactions [9, 10], though often at the cost of more model parameters. One may also just ignore the spectroscopy which is distilled from experiment, and, instead of comparing resonance positions and widths to information from the spectroscopic tables, compare the model's predictions directly, if possible, to experimental scattering cross sections and phase shifts [11, 12, 13, 14, 15, 16, 17, 18].

Here we will discuss the eternally disputed [19, 20] low-lying nonet of  $S$ -wave poles in meson-meson scattering cross sections, which are predicted by a four-parameter model [14]. It should thereby be noted that the model's parameters have already been fitted to the  $J^P = 1^- c\bar{c}$  and  $b\bar{b}$  spectra, as well as to  $P$ -wave meson-meson scattering data [13].

First, let us outline the motivation for our work. For the interaction in the vicinity of a resonance in meson-meson scattering, one may consider quark-exchange or quark-pair-creation processes, as depicted in Fig. (1). When the intermediate  $q\bar{q}$  system is close enough to a genuine bound state of confinement, then the system will resonate, resulting in a resonance in meson-meson scattering. Another picture for the same phenomenon, shown in Fig. (2), is that a mesonic quark-antiquark system (M) gets a self-energy correction from a virtual meson loop.

Either picture describes the same physical situation, namely a mesonic resonance or bound state [21], but in a rather different way. Our aim is to merge both pictures in one model.

## 1 Quark exchange

In the quark-exchange picture we obtain a resonance in the particular partial-wave meson-meson-scattering cross section which agrees with the quantum numbers of the intermediate  $q\bar{q}$  system.

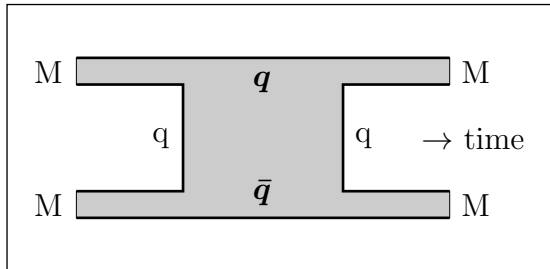


Figure 1: The mesons (M) exchange a quark or, equivalently, a quark-antiquark pair is annihilated, followed by a second quark exchange, equivalent to a new quark-antiquark pair being created.

Such a process may be described by scattering phase shifts of the form

$$\cotg(\delta_\ell(s)) \approx \frac{E_R - \sqrt{s}}{\Gamma_R/2} \quad , \quad (1)$$

where  $E_R$  and  $\Gamma_R$  represent the central invariant meson-meson mass and the resonance width, respectively.

However, formula (1) is a good approximation for the scattering cross section only when the resonance shape is not very much distorted and the width of the resonance is small. Moreover, the intermediate state in such a process is essentially a constituent  $q\bar{q}$  configuration that is part of a confinement spectrum (also referred to as bare or intrinsic states), and hence may resonate in one of the eigenstates. This implies that the colliding mesons scatter off the whole  $q\bar{q}$  confinement spectrum of radial, and possibly also angular excitations, not just off one single state [22]. Consequently, a full expression for the phase shifts of formula (1) should contain all possible eigenstates of such a spectrum as long as quantum numbers are respected. Let us denote the eigenvalues of the relevant part of the spectrum by  $E_n$  ( $n = 0, 1, 2, \dots$ ) and the

corresponding eigenstates by  $F_n$ . Then, following the procedure outlined in Ref. [23], we may write for the partial-wave phase shifts the more general expression

$$\cotg(\delta(s)) = \left[ I(s) \sum_{n=0}^{\infty} \frac{|\mathcal{F}_n|^2}{\sqrt{s} - E_n} \right]^{-1} \left[ R(s) \sum_{n=0}^{\infty} \frac{|\mathcal{F}_n|^2}{\sqrt{s} - E_n} - 1 \right] . \quad (2)$$

In  $R(s)$  and  $I(s)$  we have absorbed the kinematical factors and the details of two-meson scattering, and moreover the three-meson vertices. The details of formula (2) can be found in Ref. [23].

For an approximate description of a specific resonance and in the rather hypothetical case that the three-meson vertices have small coupling constants, one may single out, from the sum over all confinement states, one particular state (say number  $N$ ), the eigenvalue of which is nearest to the invariant meson-meson mass close to the resonance. Then, for total invariant meson-meson masses  $\sqrt{s}$  in the vicinity of  $E_N$ , one finds the approximation

$$\cotg(\delta(s)) \approx \frac{[E_N + R(s) |\mathcal{F}_N|^2] - \sqrt{s}}{I(s) |\mathcal{F}_N|^2} . \quad (3)$$

Formula (3) is indeed of the form (1), with the central resonance position and width given by

$$E_R \approx E_N + R(s) |\mathcal{F}_N|^2 \quad \text{and} \quad \Gamma_R \approx 2I(s) |\mathcal{F}_N|^2 . \quad (4)$$

In experiment one observes the influence of the nearest bound state of the confinement spectrum, as in classical resonating systems. Nevertheless, formula (3) is only a good approximation when the three-meson couplings are small. Since the coupling of the meson-meson system to quark exchange is strong, the influence of the higher- and lower-lying excitations is not negligible.

In the other hypothetical limit, namely of very large couplings, we obtain for the phase shift the expression

$$\cotg(\delta(s)) \approx \frac{R(s)}{I(s)} , \quad (5)$$

which describes scattering off an infinitely hard cavity.

The physical values of the couplings come out somewhere in between the two hypothetical cases. Most resonances and bound states can be classified as stemming from a specific confinement state [24, 25]. However, some structures in the scattering cross section stem from the cavity which is formed by quark exchange or pair creation [23]. The most notable of such states are the low-lying resonances observed in  $S$ -wave pseudoscalar-pseudoscalar scattering [26, 27, 28, 29].

## 2 Meson loops

From the discussion in Sec. (1) one may conclude that to lowest order the mass of a meson follows from the quark-antiquark confinement spectrum. It is however well-known that higher-order contributions to the meson propagator, in particular those from meson loops, cannot be neglected.

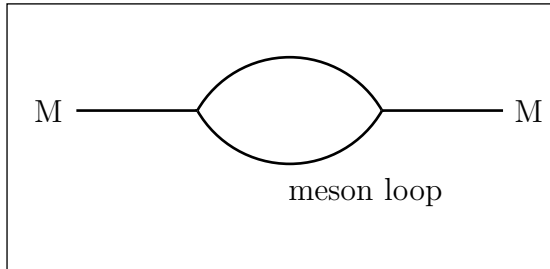


Figure 2: The lowest-order self-energy graph for a meson propagator.

Virtual meson loops give a correction to the meson mass, whereas decay channels also contribute to the strong width of the meson. One obtains for the propagator of a meson the form

$$\Pi(s) = \frac{1}{s - \left(M_{\text{confinement}} + \sum \Delta M_{\text{meson loops}}\right)^2} \quad , \quad (6)$$

where  $\Delta M$  develops complex values when open decay channels are involved.

For the full mass of a meson, all possible meson-meson loops have to be considered. A model for meson-meson scattering must therefore include all possible inelastic channels as well. Although in principle this could be done, in practice it is not manageable, unless a scheme exists dealing with all vertices and their relative intensities. In Ref. [30] relative couplings have been determined in the harmonic-oscillator approximation assuming  ${}^3P_0$  quark exchange. However, further kinematical factors must be worked out and included.

### 3 The spectrum

The complete model consists of an expression for the  $K$  matrix, similar to formula (2), but extended to many meson-meson scattering channels, several constituent quark-antiquark channels, and more complicated transition potentials [13, 14], which at the same time and with the same set of four parameters reproduces bound states, partial-wave scattering quantities, and the electromagnetic transitions of  $c\bar{c}$  and  $b\bar{b}$  systems [31].

The  $K$  matrix can be analytically continued below the various thresholds, even the lowest one, with no need of redefining any of the functions involved, in order to study the singularities of the corresponding scattering matrix. Below the lowest threshold, these poles show up on the real  $\sqrt{s}$  axis, and can be interpreted as the bound states of the coupled system, to be identified with the stable mesons. For the light flavours one finds this way a nonet of light pseudoscalars, i.e., the pion, Kaon, eta, and eta'. For the heavy flavours, the lowest-lying model poles can be identified with the  $D(1870)$ ,  $D_s(1970)$ ,  $\eta_c(1S)$ ,  $J/\psi(1S)$ ,  $\psi(3686)$ ,  $B(5280)$ ,  $B_s(5380)$ ,  $\Upsilon(1S)$ ,  $\Upsilon(2S)$ , and  $\Upsilon(3S)$ .

Above the lowest threshold, the model's partial-wave cross sections and phase shifts for all included meson-meson channels can be calculated and compared to experiment, as well as the inelastic transitions. Singularities of the scattering matrix come out with negative imaginary part in the  $\sqrt{s}$  plane. To say it more precisely: out of the many singularities in a rather complex set of Riemann sheets, some come close enough to the physical real axis to be noticed in the partial-wave phase shifts and cross sections. In fact, each meson-meson channel doubles

the number of Riemann sheets, hence the number of poles. Consequently, with ten scattering channels one has for each eigenvalue of the confinement spectrum 1024 poles in 1024 Riemann sheets, out of which usually only one contains relevant poles in each  $\sqrt{s}$  interval in between the thresholds. Those can be identified with the known resonances, like the  $\rho$  pole in  $\pi\pi$  scattering, or the  $K^*$  pole in  $K\pi$  scattering. However, there might always be a pole in a nearby Riemann sheet just around the corner of one of the thresholds, which can be noticed in the partial-wave cross section. The study of poles is an interesting subject by itself [32, 33].

Once the four model parameters have been adjusted to the experimental phase shifts and cross sections, the pole positions can be determined and compared to tables for meson spectroscopy. But usually no new information is gained from such a comparison. Here we will report on the singularity structure of the lowest poles in  $S$ -wave meson-meson scattering.

## 4 Scattering-matrix poles

In the hypothetical case of very small couplings for the three-meson vertices, we obtain poles in the scattering matrix that are close to the eigenvalues of the confinement spectrum. Let us denote by  $M_1$  and  $M_2$  the meson masses, and by  $\Delta E$  the difference between the complex-energy pole of the scattering matrix and the energy eigenvalue,  $E_N$ , of the nearby state of the confinement spectrum. Using formula (4), we obtain

$$\Delta E \approx \{R(s) - iI(s)\} |\mathcal{F}_N|^2 \quad . \quad (7)$$

We may distinguish two different cases:

- (1)  $E_N > M_1 + M_2$  (above threshold),
- (2)  $E_N < M_1 + M_2$  (below threshold).

When the nearby state of the confinement spectrum is in the scattering continuum, then  $\Delta E$  has a **negative** imaginary part and a real part, since both  $R(s)$  and  $I(s)$  of formula (7) are real, and  $I(s)$  is moreover positive. The resonance singularity of the scattering matrix which corresponds to this situation is depicted in Fig. (3).

Notice that the resonance singularity is in the lower half of the complex-energy plane (second Riemann sheet), as it should be.

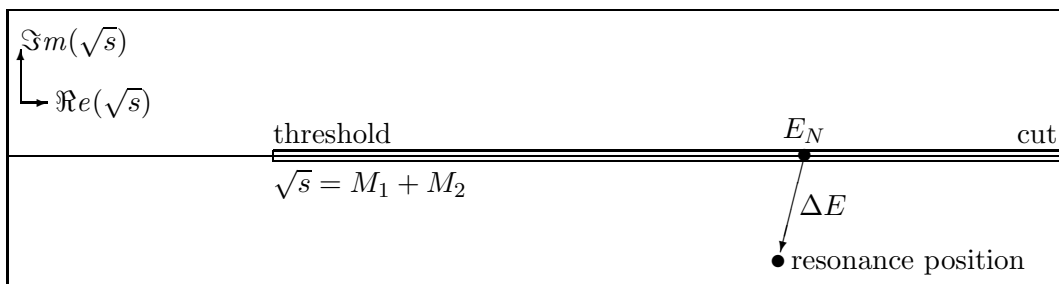


Figure 3: When the confinement state on the real  $\sqrt{s}$  axis is in the scattering continuum, then for small coupling (perturbative regime) the resonance pole moves into the lower half of the complex  $\sqrt{s}$  plane.

When the nearby state of the confinement spectrum is below the scattering threshold, then  $\Delta E$  has only a real part, since  $I(s)$  turns purely imaginary below threshold, whereas  $R(s)$  remains real. The bound-state singularity of the scattering matrix corresponding to this situation is depicted in Fig. (4).

Note that the bound-state pole is on the real axis of the complex-energy plane, as it should be.

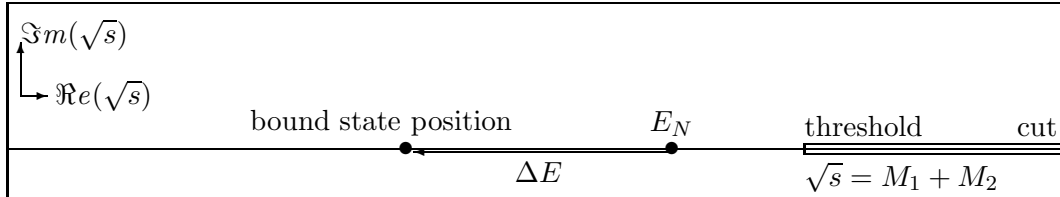


Figure 4: When the confinement state on the real  $\sqrt{s}$  axis is below the lowest scattering threshold, then the bound-state singularity comes out on the real  $\sqrt{s}$  axis.

## 5 Threshold behaviour

Near the lowest threshold, as a function of the overall coupling constant,  $S$ -wave poles behave very differently from  $P$ - and higher-wave poles. This can easily be understood from the effective-range expansion [34] at the pole position. There, the cotangent of the phase shift equals  $i$ . Hence, for  $S$  waves the next-to-lowest-order term in the expansion equals  $ik$  ( $k$  represents the linear momentum related to  $s$  and to the lowest threshold). For higher waves, on the other hand, the next-to-lowest-order term in the effective-range expansion is proportional to  $k^2$ .

Poles for  $P$  and higher waves behave in the complex  $k$  plane as indicated in Fig. (5b). The two  $k$ -plane poles meet at threshold ( $k = 0$ ). When the coupling constant of the model is increased, the poles move along the imaginary  $k$  axis. One pole moves towards negative imaginary  $k$ , corresponding to a virtual bound state below threshold on the real  $\sqrt{s}$  axis, but in the wrong Riemann sheet. The other pole moves towards positive imaginary  $k$ , corresponding to a real bound state.

For  $S$ -wave poles, the behaviour is shown in Fig. (5a). The two  $k$ -plane poles meet on the negative imaginary  $k$  axis. When the coupling constant of the model is slightly increased, both poles continue on the negative imaginary  $k$  axis, corresponding to two virtual bound states below threshold on the real  $\sqrt{s}$  axis. Upon further increasing the coupling constant of the model, one pole moves towards increasing negative imaginary  $k$ , thereby remaining a virtual bound state for all values of the coupling constant. The other pole moves towards positive imaginary  $k$ , eventually passing threshold ( $k = 0$ ), thereby turning into a real bound state of the system of coupled meson-meson scattering channels. Hence, for a small range of hypothetical values of the coupling constant, there are two virtual bound states, one of which is very close to threshold. Such a pole certainly has noticeable influence on the scattering cross section.

Although we are not aware of any experimental data that could confirm the above-described threshold behaviour of poles, we suspect this to be possible for atomic transitions in cavities. Unfortunately, it does not seem likely that in the near future similar processes can be studied for strong coupling.

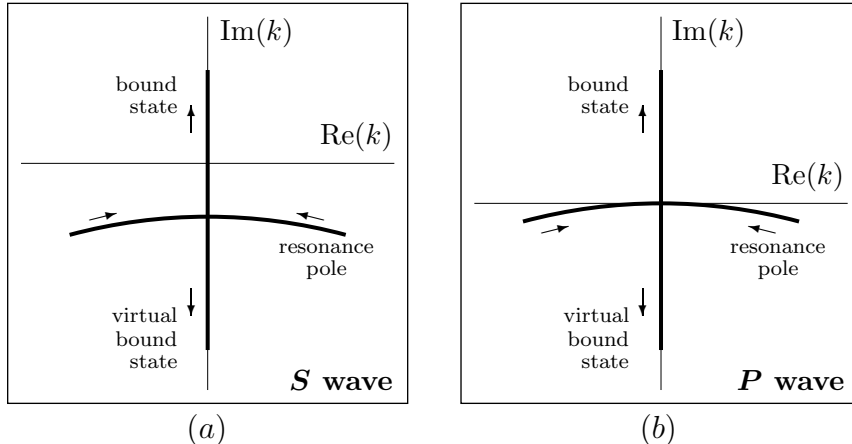


Figure 5: Variation of the positions of scattering-matrix poles as a function of hypothetical variations in the three-meson-vertex coupling, for  $S$  waves (a), and for  $P$  and higher waves (b). The arrows indicate increasing coupling constant.

## 6 The low-lying nonet of $S$ -wave poles

The nonet of low-lying  $S$ -wave poles behave as described in Sec. (4), with respect to variations of the model's overall coupling constant. However, they do not stem from the confinement spectrum, but rather from the cavity. For small values of the coupling, such poles disappear into the continuum, i.e., they move towards negative imaginary infinity [23], and not towards an eigenstate of the confinement spectrum as in Fig. (3).

In Fig. (6) we study the hypothetical pole positions of the  $K_0^*(730)$  pole in  $K\pi$   $S$ -wave scattering. The physical value of the coupling constant equals 0.75, which is not shown in Fig. (6). A figure for smaller values of the coupling constants can be found in Ref. [23]. The physical pole in  $K\pi$  isodoublet  $S$ -wave scattering, related to experiment [28, 27], comes out at  $727 - i263$  MeV in Ref. [14]. Here we concentrate on the threshold behaviour of the hypothetical pole movements in the complex  $k$  and  $\sqrt{s}$  planes. Until they meet on the axis, which is for a value of the coupling constant slightly larger than 1.24, we have only depicted the right-hand branch.

In the left figure we observe how the poles arrive on the imaginary  $k$  axis, and then continue to move along that axis. One of the poles moves upwards, initially describing a virtual bound state, and crossing the real  $k$  axis for a value of the coupling constant slightly larger than 1.30. The other pole moves downwards, remaining a virtual bound state for further increasing values of the coupling constant.

In the right figure the same pole has been depicted in the  $\sqrt{s}$  plane. Here, the situation is more confusing, since the pole positions are in the same interval of energies. The pole which corresponds to the one moving downwards along the imaginary  $k$  axis moves to the left on the real  $\sqrt{s}$  axis. Its positions as a function of the coupling constant are indicated by solid circles. The pole which moves upwards along the imaginary  $k$  axis initially moves towards threshold and then turns back, following the former pole, but in a different Riemann sheet. The positions of the latter pole are indicated by open circles. In the inset we try to better clarify its motion. Notice that, since we took 0.14 GeV and 0.50 GeV for the pion and the Kaon mass, respectively, we end up with a threshold at 0.64 GeV.

It is interesting to notice that in a recent work of M. Boglione and M.R. Pennington [35]

also a zero-width state is found below the  $K\pi$  threshold in  $S$ -wave scattering. Here, we obtain such a state for *unphysical* values of the coupling.

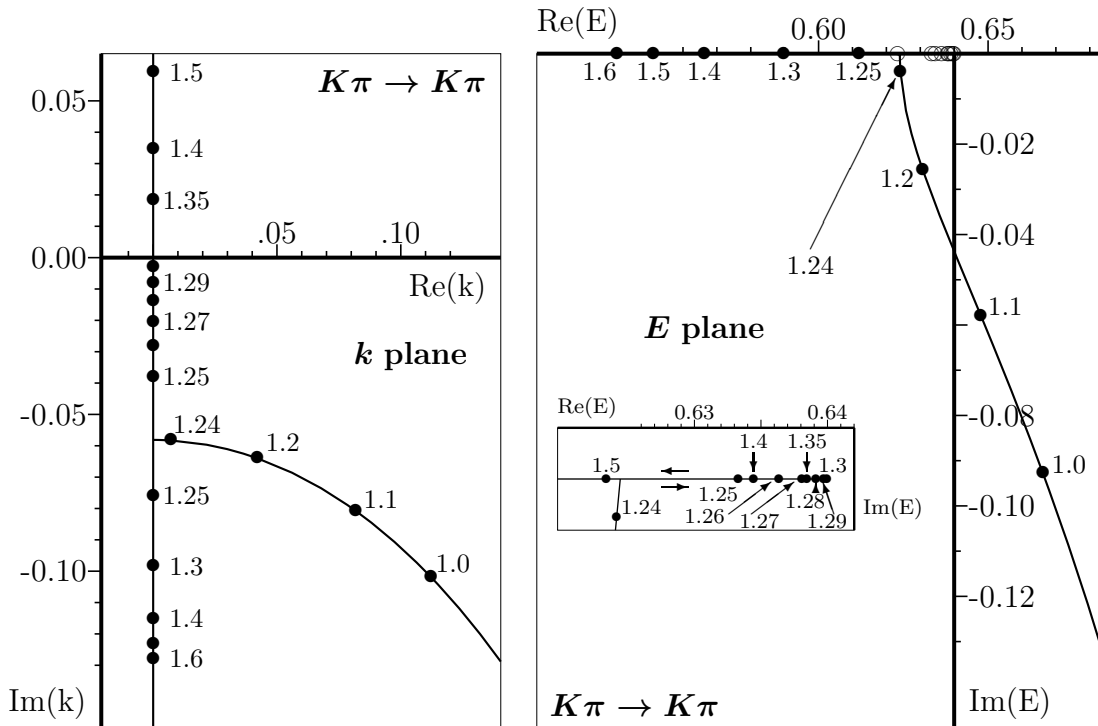


Figure 6: Hypothetical movement of the  $K_0^*(730)$  pole in  $K\pi$   $S$ -wave scattering as a function of the coupling constant. The two branches on the imaginary  $k$  axis are discussed in the text. In the  $E = \sqrt{s}$  plane these two branches come out on the real axis below threshold. The poles of the upper branch are shown as open circles in the main figure, and as closed circles in the inset. Units are in GeVs.

In Fig. (7) we have depicted the movement of the  $a_0(980)$  pole in  $S$  wave  $I = 1$   $KK$  scattering (threshold at 1.0 GeV) on the upwards-going branch. One observes a very similar behaviour as in the case of  $K\pi$  scattering, but with two important differences, to be described next.

The  $K_0^*(730)$  poles meet on the real  $\sqrt{s}$  axis only 16 MeV below threshold (see Fig. 6), and for a value of the coupling constant which is well above the physical value of 0.75, whereas the  $a_0(980)$  poles meet 238 MeV below threshold, when the coupling constant only equals 0.51. At the physical value of the coupling constant, the  $a_0(980)$  pole is a real bound state some 9 MeV below threshold.

But there is yet another difference. Whereas the  $K\pi$  channel represents the lowest possible scattering threshold for the  $K_0^*(730)$  system,  $KK$  is not the lowest channel for the  $a_0(980)$ . In a more complete description, at least all pseudoscalar meson-meson loops should be taken into account. One of these is the  $\eta\pi$  channel, which has a threshold well below  $KK$ . Consequently, upon including the  $\eta\pi$  channel in the model, the pole cannot remain on the real  $\sqrt{s}$  axis, but has to acquire an imaginary part in a similar way as shown in Fig. (3). In Ref. [14] we obtained a resonance-like structure in the  $\eta\pi$  cross section, representing the physical  $a_0(980)$ . The corresponding pole came out at  $962 - i28$  MeV.

For the  $f_0(980)$  system the situation is very similar to that of the  $a_0(980)$ . Assuming a pure



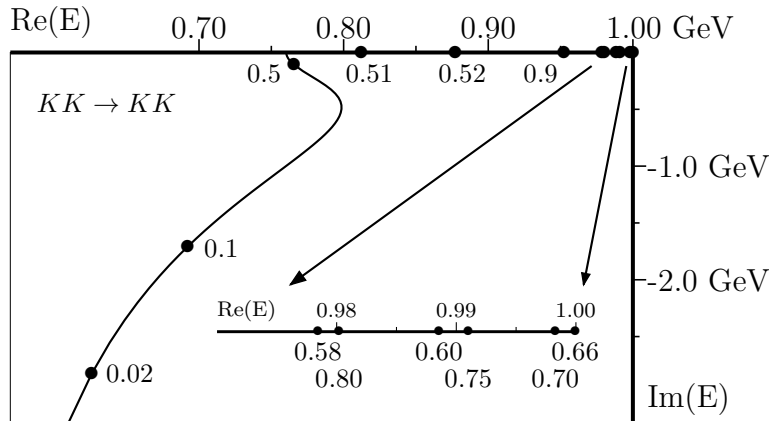


Figure 7: Pole movement as a function of the coupling constant for  $KK$   $I = 1$   $S$ -wave scattering. Some values of the coupling constant are indicated in the figure. The six filled circles at the right end of the real axis correspond, from left to right, to the values 0.58, 0.80, 0.60, 0.75, 0.70, and 0.66 for the model's coupling constant. This situation is magnified in the inset.

$s\bar{s}$  quark content [36], we obtain for the variation of the corresponding pole in  $KK$   $I = 0$   $S$ -wave scattering a picture almost equal to the one shown in Fig. (7). However, only in lowest order the  $KK$  channel could be considered the lowest threshold for the  $f_0(980)$  system. In reality  $s\bar{s}$  also couples to the nonstrange quark-antiquark isosinglet through  $KK$ , and hence to  $\pi\pi$  [15]. This coupling is nevertheless very weak, which implies that the resulting pole does not move far away from the  $KK$  bound state. In Ref. [14] we obtained a resonance-like structure in the  $\pi\pi$  cross section representing the physical  $f_0(980)$ . The corresponding pole came out at  $994 - i20$  MeV.

At lower energies, we found for the same cross section a pole which is the equivalent of the  $K_0^*(730)$  system, but now in  $\pi\pi\pi$  isoscalar  $S$ -wave scattering. This pole at  $470 - i208$  MeV may be associated with the  $\sigma$  meson, since it has the same quantum numbers and lies in the ballpark of predicted pole positions in  $\sigma$  models (for a complete overview of  $\sigma$  poles, see Ref. [37]).

We do not find any other relevant poles in the energy region up to 1.0 GeV.

## 7 Conclusions

We have shown that the poles of the  $a_0(980)$  and  $f_0(980)$  belong to a nonet of scattering-matrix poles. The lower-lying isoscalar pole and the isodoublet poles in the complex-energy plane have real parts of 0.47 GeV and 0.73 GeV, respectively, and imaginary parts of 0.21 GeV resp. 0.26 GeV. Whether these poles represent real physical resonances [38] is not so relevant here. Important is that the  $a_0(980)$  and  $f_0(980)$  are well classified within a nonet of scattering-matrix poles with very specific characteristics, different from those of the poles stemming from confinement, like the confinement-ground-state nonet of scalar mesons  $f_0(1370)$ ,  $a_0(1450)$ ,  $K_0^*(1430)$ , and  $f_0(1500)$ . The latter poles vary as a function of the coupling constant exactly the way indicated in figure (3). For vanishing coupling constant they end up on the real  $\sqrt{s}$  axis at the positions of the various ground-state eigenvalues of the confinement spectrum, which are the light-flavour  $^3P_0$  states at 1.3 to 1.5 GeV [39, 40, 41].

The low-lying  $S$ -wave poles related to the cross sections in the  $f_0(470)$ ,  $K_0^*(730)$ ,  $f_0(980)$ , and  $a_0(980)$  regions move to negative imaginary infinity in the  $\sqrt{s}$  plane for decreasing values of the coupling. The pole positions for the physical value of the coupling are well explained by their threshold behaviour. Whether or not these poles have large imaginary parts, leading to large widths and strong resonance distortion, depends in a subtle way on the thresholds and couplings of the various relevant scattering channels [42].

As to the nature of the light scalar mesons, which has recently been discussed in Refs. [19, 20, 43, 44], we can only remark that in a many-coupled-channel model each of the channels contributes to the states under the resonance, not just one specific channel.

Comparing to experiment cross sections and phase shifts that follow from modelling strong interactions is a particularly useful strategy, since then the model gains independence with respect to the criteria for omitting experimental results from the spectroscopic tables [45, 46]. Moreover, this strategy has another advantage. Phase shifts do not easily follow from confinement models, nor does Nature provide a bound-state spectrum of mesons. Confinement models and spectroscopic tables go well together, but do not shed sufficient light on strong interactions. Both can be avoided when following the strategy outlined above. Nonetheless, it would be useful to have some coordination in the availability of experimental results on meson-meson scattering.

**Acknowledgement:** We wish to thank Frieder Kleefeld for useful discussions on the distribution of  $S$ -matrix poles in the complex  $E$  and  $k$  planes.

This work has been partly supported by the *Fundação para a Ciência e a Tecnologia* of the *Ministério da Ciência e da Tecnologia* of Portugal, under contract numbers POCTI/35304/FIS/2000, and CERN/P/FIS/40119/2000.

## References

- [1] J. Vijande, F. Fernández, A. Valcarce, B. Silvestre-Brac, arXiv:hep-ph/0206263.
- [2] Stephen Godfrey and Nathan Isgur, Phys. Rev. D **32** (1985) 189.
- [3] A. Donnachie and A. B. Clegg, Z. Phys. C **51** (1991) 689.
- [4] A. Donnachie, CERN-TH-5246-88 *Invited talk given at 'Fenice' Workshop, Frascati, Italy, Oct 27-28, 1988.*
- [5] D. Aston *et al.*, Nucl. Phys. Proc. Suppl. **21** (1991) 105.
- [6] D. Aston *et al.*, SLAC-PUB-5721 *Invited talk given at Int. Conf. on Hadron Spectroscopy, College Park, MD, Aug 12-16, 1991.*
- [7] W. M. Dunwoodie, P. Rensing and L. Chen [LASS Collaboration], SLAC-PUB-5675 *Presented at Joint Inst. Lepton-Photon Symp. and Europhysics Conf. on High Energy Physics, Geneva, Switzerland, Jul 25 - Aug 1, 1991.*
- [8] D. Aston *et al.*, SLAC-PUB-5657 *Presented at Particles and Fields '91, Vancouver, Canada, Aug 18-22, 1991.*
- [9] V. Bernard, A. H. Blin, B. Hiller, Y. P. Ivanov, A. A. Osipov and U. G. Meissner, Phys. Lett. B **409** (1997) 483 [arXiv:hep-ph/9705438].

- [10] R. Ricken, M. Koll, D. Merten, B. C. Metsch and H. R. Petry, Eur. Phys. J. A **9** (2000) 221 [arXiv:hep-ph/0008221].
- [11] E. Eichten, In *\*Cargese 1975, Proceedings, Weak and Electromagnetic Interactions At High Energies, Part A\**, New York 1976, 305-328.
- [12] E. Eichten, K. Gottfried, T. Kinoshita, K. D. Lane and T. M. Yan, Phys. Rev. D **21**, 203 (1980).
- [13] E. van Beveren, G. Rupp, T. A. Rijken, and C. Dullemond, Phys. Rev. **D27** (1983) 1527.
- [14] E. van Beveren, T. A. Rijken, K. Metzger, C. Dullemond, G. Rupp and J. E. Ribeiro, Z. Phys. **C30** (1986) 615.
- [15] R. N. Cahn and P. V. Landshoff, Nucl. Phys. B **266** (1986) 451.
- [16] Nils A. Törnqvist and Matts Roos, Phys. Rev. Lett. **76** (1996) 1575 [arXiv:hep-ph/9511210].
- [17] Frank E. Close, arXiv:hep-ph/0110081.
- [18] Agnieszka Furman and Leonard Leśniak, arXiv:hep-ph/0203255.
- [19] Frank E. Close and Nils A. Törnqvist, arXiv:hep-ph/0204205.
- [20] Nils A. Törnqvist, arXiv:hep-ph/0201171.
- [21] Frank E. Close and Nathan Isgur, Phys. Lett. B **509** (2001) 81 [arXiv:hep-ph/0102067].
- [22] Tullio Regge, Nuovo Cim. **14** (1959) 951.
- [23] Eef van Beveren and George Rupp, Eur. Phys. J. **C22**, 493 (2001) [arXiv:hep-ex/0106077].
- [24] A. V. Anisovich and A. V. Sarantsev, Phys. Lett. **B413** (1997) 137 [arXiv:hep-ph/9705401].
- [25] V. V. Anisovich and A. V. Sarantsev, arXiv:hep-ph/0204328.
- [26] Carla Göbel, on behalf of the E791 Collaboration, Proceedings of Heavy Quarks at Fixed Target (HQ2K), Rio de Janeiro, October 2000, 373-384, hep-ex/0012009;
- [27] Carla Göbel, on behalf of the E791 Collaboration, To appear in the proceedings of 9th International Conference on Hadron Spectroscopy (Hadron 2001), Protvino, Russia, 25 Aug - 1 Sep 2001, arXiv:hep-ex/0110052.
- [28] E. M. Aitala *et al.* [E791 Collaboration], arXiv:hep-ex/0204018.
- [29] Eef van Beveren and George Rupp, talk given at HADRON 2001, Protvino, Russia, August 2001, arXiv:hep-ph/0110156.
- [30] E. van Beveren, Z. Phys. **C21** (1984) 291.
- [31] A. G. Verschuren, C. Dullemond, and E. van Beveren, Phys. Rev. **D44** (1991) 2803.

- [32] Matthias Jamin, José Antonio Oller, and Antonio Pich, Nucl. Phys. **B587**, 331 (2000) [hep-ph/0006045].
- [33] J. A. Oller, E. Oset and J. R. Peláez, Phys. Rev. **D59** (1999) 074001 [Erratum-ibid. **D60** (1999) 099906] [arXiv:hep-ph/9804209].
- [34] V. De Alfaro and T. Regge, *Potential Scattering*, North Holland (Amsterdam, 1965).
- [35] M. Boglione and M. R. Pennington, arXiv:hep-ph/0203149.
- [36] F. De Fazio and M. R. Pennington, Phys. Lett. B **521** (2001) 15 [arXiv:hep-ph/0104289].
- [37] Eef van Beveren and George Rupp, arXiv:hep-ph/0201006.
- [38] S. N. Cherry and M. R. Pennington, Nucl. Phys. A **688** (2001) 823 [arXiv:hep-ph/0005208].
- [39] W. Lee and D. Weingarten, Phys. Rev. **D61**, 014015 (2000) [hep-lat/9910008]; D. Weingarten, private communication.
- [40] W. Lee and D. Weingarten, hep-lat/9805029.
- [41] W. Lee and D. Weingarten, Nucl. Phys. Proc. Suppl. **53**, 236 (1997) [hep-lat/9608071].
- [42] Kim Maltman, Phys. Lett. **B462** (1999) 14 [arXiv:hep-ph/9906267].
- [43] Kim Maltman, Nucl. Phys. **A675** (2000) 209c.
- [44] C. M. Shakin, Phys. Rev. D **65** (2002) 114011.
- [45] T. Barnes, *Hadron 2001 conference summary: Theory*, Presented at 9th International Conference on Hadron Spectroscopy (Hadron 2001), Protvino, Russia, 25 Aug - 1 Sep 2001, arXiv:hep-ph/0202157.
- [46] E. Klempt, *Hadron 2001 conference summary: Experiment*, Presented at 9th International Conference on Hadron Spectroscopy (Hadron 2001), Protvino, Russia, 25 Aug - 1 Sep 2001.